A Novel Multi-functional Polymeric Curing Agent: Synthesis, Characterization, and Its Epoxy Resin with Simultaneous Excellent Flame Retardance and Transparency

Zhu-Bao Shao, Ming-Xin Zhang, Ying Li, Ye Han, Liang Ren, Cong Deng

PII: S1385-8947(18)30500-X
DOI: https://doi.org/10.1016/j.cej.2018.03.142
Reference: CEJ 18749

To appear in: *Chemical Engineering Journal*

Received Date: 13 December 2017
Revised Date: 24 February 2018
Accepted Date: 26 March 2018

Please cite this article as: Z-B. Shao, M-X. Zhang, Y. Li, Y. Han, L. Ren, C. Deng, A Novel Multi-functional Polymeric Curing Agent: Synthesis, Characterization, and Its Epoxy Resin with Simultaneous Excellent Flame Retardance and Transparency, *Chemical Engineering Journal* (2018), doi: https://doi.org/10.1016/j.cej.2018.03.142

A Novel Multi-functional Polymeric Curing Agent: Synthesis, Characterization, and Its Epoxy Resin with Simultaneous Excellent Flame Retardance and Transparency

Zhu-Bao Shao[a], *Ming-Xin Zhang*[a], *Ying Li*[b], *Ye Han*[a], *Liang Ren*[a*] *and Cong Deng*[c*]

[a]*Institute of Chemical Engineering, Changchun University of Technology, Changchun 130012, China*

[b]*Key Laboratory of Polymer Eco-materials, Changchun Institute of Applied Chemistry, Chinese Academy of Sciences, Changchun 130022, People's Republic of China*

[c]*National Engineering Laboratory of Eco-Friendly Polymeric Materials (Sichuan); Analytical and Testing Center, Sichuan University, Chengdu 610064, China*

Abstract: Traditional cured epoxy resin (EP) usually loses its transparency once it encounters the requirement of flame retardance. To obtain the EP with simultaneous excellent transparency and flame retardancy, a novel multi-functional polymeric curing agent named DPPEI was synthesized via a reaction between diphenylphosphinic chloride (DPPC) and polyethylenimine (PEI) in this work. Different measurements confirmed that the DPPEI was prepared successfully. After incorporation of the DPPEI into EP, the cured EP (DPPEI-EP) material with simultaneous excellent transmittance and flame retardancy was

Corresponding author: Tel. & Fax: +86-28-85410259.

E-mail address: dengcong@scu.edu.cn (C. Deng)

obtained after a mild curing process. The transmittance of the resulting DPPEI-EP was kept at about 90% in the visible region at a loading of 35 wt% DPPEI, meanwhile, the DPPEI-EP sample with the thickness of only 1.6 mm passed the V-0 rating in vertical burning test, had no dripping, and achieved the limiting oxygen index of 29.8%. In combustion test, both total heat release and total smoke production of the DPPEI-EP containing 30 wt% DPPEI were respectively greatly decreased by 69.5% and 78.3% compared with the corresponding value of the reference sample PEI-EP, showing high flame-retarding and smoke-suppressing efficiency. The transparent and flame-retardant mechanisms of DPPEI-EP were investigated insightfully through different tests. All these results demonstrate that the DPPEI is a novel multi-functional polymeric curing agent for EP, which has efficient curing ability and meanwhile endows the cured EP with simultaneous excellent flame retardancy and transparency.

Keywords: curing agent; flame retardant; transparency; epoxy resin

Graphical abstract

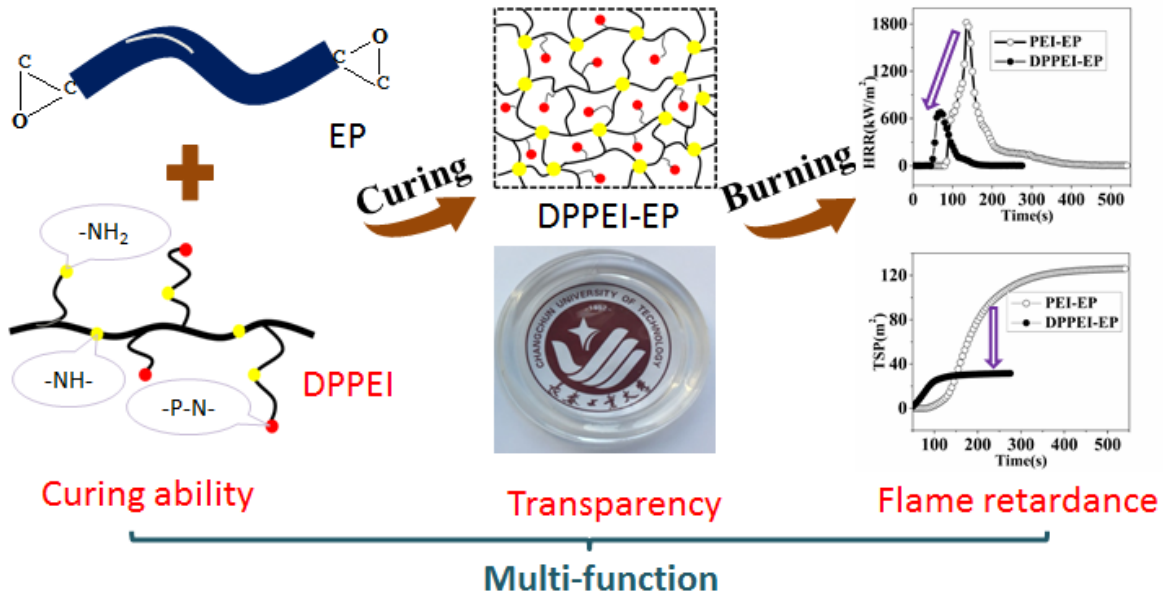

1. Introduction

Traditional EP material has been widely used in composite material, machine, coating, and electronic packaging material etc. fields because of its outstanding chemical resistance, thermal stability, mechanical and adhesive properties in the past decades.[1-6] However, its easy ignition and combustion always restrict further application in some new fields.[7-9] Moreover, in special fields such as multi-functional gradient coating, light-emitting diodes (LEDs), arts, etc., there is the requirement of simultaneous transparency and flame retardance, so the application of traditional EP material is further limited.

Much research has been done to solve the easy flammability of EP.[10-14] Generally, incorporation of inorganic or organic additive-type flame retardant is an efficient method to improve the flame retardancy of EP.[15-17] Hu et al.[18] reported that a novel polyphosphazene (PZS) microsphere@molybdenum disulfide nanoflower (MoS_2) hierarchical hybrid architecture was synthesized and applied for enhancing the flame retardancy of EP, and the result showed that the incorporation of 3 wt % PZS@MoS_2 brought about a 41.3% maximum reduction in the peak of heat release rate and decreased by 30.3% maximum in the total heat release. In addition, some flame retardants containing phosphorus were also used to flame retard the EP. [19-20] In Wang et al' s work, [21] the ammonium polyphosphate was used to flame retard the EP, and they found that the flame retardant containing phosphorus enhanced the flame retardancy of epoxy resin.

Unfortunately, incorporation of inorganic or organic additive-type flame retardants is not an ideal approach because of their bad distribution in EP and great damage to the mechanical properties of EP. To avoid the above two drawbacks, incorporation of the

phosphorus into the crosslinking network of EP has been the most popular approach. The most advantage of this method is that it may endow the cured EP material with intrinsic flame retardancy. For example, organic-modified ammonium polyphosphate (APP),[1,22] 9,10-dihydro-9-oxa-10-phosphaphenanthrene-10-oxide (DOPO), and its derivative[23-27] were used to prepare flame-retarded EPs, and these EPs displayed low smoke, excellent flame retardancy, and high thermal stability. However, they are not transparent or their transmittances are very low in most cases. To obtain transparent cured EP materials, small molecular curing agents such as thiol curing agent, amine curing agent, anhydride curing agent, etc., were used in past work,[28-29] whereas these prepared EP materials are flammable. Until now, although some progress has been made in preparing flame-retarded or transparent EP, there is still no apparent progress in preparing the EP with simultaneous excellent transparency and flame retardance in the past decades. However, on the basis of its potential great application value, the related research seems particularly significant.

The EP with excellent flame retardancy and high transmittance was rarely reported in the past work. Lin and co-workers[30] reported a curing agent hydroxyl-PES-1 and used it to endow the EP with simultaneous flame retardancy and transparency. The cured EP/hydroxyl-PES-1 containing 3.4 wt% phosphorus achieved the UL-94 V-0 rating (3.2 mm) and a light transmittance above 80% in the visible region. In this work, the preparation of hydroxyl-PES-1 is very complex, and the yield is below 38.5%. Luo et al.[31] synthesized a novel curing agent named tris(2-mercaptoethyl) phosphate (TMEP), and they found that the cured EP/TMEP with 2.7 wt% phosphorus passed the UL-94 V-0 rating, and its light transmittance was greater than 92%. During the curing process of EP/TMEP, the TMEP

could not be used alone as a curing agent for EP because of the flexibility of thioether bond, and therefore the curing process of EP must be aided by another curing agent. According to the previous work, it is known that some shortcomings still exist for multi-functional curing agents which may endow the cured EP with simultaneous flame retardancy and transparency.

To obtain the EP with simultaneous excellent flame retardancy and transparency, a novel polymeric curing agent DPPEI was successfully prepared in this work. The chemical structure of DPPEI was confirmed by ^{1}H nuclear magnetic resonance, ^{31}P nuclear magnetic resonance, X-ray photoelectron spectroscopy, and elemental analysis. After incorporation of the DPPEI into EP, the flame retardancy and transparency of the resulting DPPEI-EP were investigated through various measurements. Moreover, the transparent and flame-retardant mechanisms of DPPEI-EP were also studied insightfully.

2. Experimental section

2.1. Materials

Epoxy resin (E-51, the epoxy value of 0.51 mol/100g) was supplied by Nantong Xingchen Synthetic Material Co., Ltd. (China), and it was used as received; diphenylphosphinyl chloride (DPPC) was obtained from Shanghai Changgen Chemical Reagent Co., Ltd. (China); polyethylenimine (PEI, M_w = 600) was purchased from Shanghai Titan Scientific Co., Ltd. (China), and its amine value is about 19 (KOH) mg/g; Chloroform and sodium carbonate were provided by Tianjin Xintong Chemical Reagent Co., Ltd. (China).

2.2. Measurements

Fourier transform infrared spectroscopy (FTIR) test was performed on a Nicolet FTIR 170SX spectrometer (Nicolet, America) using the KBr disk, and the wave number range was set from 4000-400 cm^{-1}.

^{1}H nuclear magnetic resonance (^{1}H-NMR) and ^{31}P nuclear magnetic resonance (^{31}P-NMR) spectra were recorded on a Bruker AV II-400 MHz spectrometer (*Bruker*, Switzerland) using $CDCl_3$ as the solvent.

X-ray photoelectron spectroscopy (XPS) spectra were recorded by a XSAM80 instrument (Kratos Co, UK) equipped with Al Ka excitation radiation (hv-1486.6 eV), and the used analysis software is the XPSPEAK41.

Phosphorus contents of samples were determined by inductively coupled plasma-atomic emission spectrometry (ICP-AES) (IRIS Advantage, TJA solution, USA). For DPPEI, 50 mg DPPEI was added in 5% HCl solution (25 mL). After 48 h, the solution was diluted to 100 mL using the deionized water. For DPPIP-EP, 100 mg sample was completely combusted into gas under sufficient oxygen atmosphere, and the gas was absorbed by 25 mL of 0.001 mol/L $KMnO_4$/KOH solution, then diluted to 100 mL using the deionized water.

Scanning electronic microscopy (SEM, JEOL JSM 5900LV, Japan) was used to analyze the cured EP and its residues after combustion under an accelerating voltage of 20 kV, and an energy dispersive X-ray spectrometer (EDX) was equipped for elemental analysis.

UV-Vis Transmittance spectra (SHIMADZU, Japan) of samples with the thickness of 1.0 mm was recorded through a UV1800 UV-Vis scanning spectrophotometer.

The X-ray diffraction (XRD) test using Cu Kα radiation (λ=1.542 Å) was performed on a power DX-1000 diffractometer (Dandong Fangyuan, China) under the scanning rate of

0.02°/s in the 2θ range of 5-50°.

Dynamic mechanical analysis was performed using a DMA Q 800 apparatus (TA, USA) under the constant frequency of 1.0 Hz, oscillation amplitude of 10.0 μm, and heating rate of 5 °C/min in a three-point bending model. The dimension of specimens for DMA test is 40 mm × 10 mm × 4 mm.

Tensile test was completed under a crosshead speed of 20 mm/min according to the procedure in GB/T 1040.1-2006. The Izod impact property was tested according to the procedure in GB/T 1843-2008 and the depth of nick was 4 mm. Flexural test was performed under the speed of 10 mm/min according to GB/T 9341-2008 at room temperature.

Thermogravimetric (TG) analysis was carried out by a TG 209F1 (NETZSCH, Germany) thermogravimetric analyzer at a heating rate of 10 °C/min in the temperature range from 40 to 700 °C under nitrogen flow of 50 mL/min.

The limited oxygen index (LOI) value was measured using an HC-2C oxygen index instrument (Jiangning, China) according to ASTM D2863-97. The dimension of all samples is 130 mm × 6.5 mm × 3.2 mm.

The UL-94 vertical burning level was tested on a CZF-2 instrument (Jiangning, China) according to ASTM D 3801. The dimension of samples is 130 mm × 13 mm × 3.2 (1.6) mm.

The flammability of samples was measured by a cone calorimeter (CC) device (Fire Testing Technology, UK). The samples with the dimension of 100 mm × 100 mm × 3 mm were exposed to a radiant cone under a heat flux of 35 kW/m^2.

Thermogravimetry-Fourier transform infrared spectroscopy (TG-FTIR) consists of a TG 209 F1 (NETZSCH, Germany) and a 170 SX FTIR spectrometer (Nicolet, America). A

sample (about 6 mg) was heated at a rate of 10 °C/min in the temperature range from 40 to 700 °C under nitrogen flow of 50 mL/min.

2.3. Synthesis of the DPPEI

The synthetic process of the DPPEI is shown in **Scheme 1**. First, 20 g (0.03 mol) PEI, 10 g sodium carbonate, and 100 ml chloroform were mixed in a three-necked round-bottom flask with a reflux condenser at about 20 °C under nitrogen atmosphere. Then, 60 ml chloroform containing 15 g (0.06 mol) DPPC was dropped into the above mixed solution in 1 h. Subsequently, the solution was kept at 20 °C for 2 h. After the reaction, the mixed solution was filtered, and the transparent solid DPPEI was obtained. Here, the yield of DPPEI was 90.5%. According to the calculation, the active hydrogen equivalent weight of DPPEI is about 57.3.

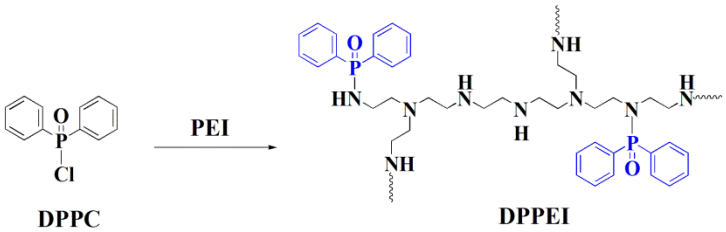

DPPC DPPEI

Scheme 1. The synthetic route of DPPEI.

2.4. Curing process of the EP

Formulations of the DPPEI-EPs and the reference sample PEI-EP are listed in **Table 1**. The number in the sample name represents the weight ratio of the DPPEI in the DPPEI-EP. The cured DPPEI-EPs with different contents of DPPEI were prepared according to the following process. First, the DPPEI was added into 100 mL chloroform in which there was 50.0 g EP, accompanied by continuously stirring. The mixed solution of DPPEI and EP was steadily stirred at 20 °C for 10 min until the solution of EP/DPPEI became homogeneous.

Then, the mixed solution was poured into a prepared mould and cured at 25 ℃ for 10 min under vacuum. Successively, the mixture was transferred in an air-circulating oven and followed by a step-curing process at 56 ℃ for 1 h and 80 ℃ for 2 h. For the PEI-EP, the preparation process is the same as that of DPPEI-EP. According to the calculation, the equivalent ratio of epoxy and active hydrogen for PEI-EP, DPPEI(20)-EP, DPPEI(25)-EP, DPPEI(30)-EP, and DPPEI(35)-EP are 0.38, 1.17, 0.87, 0.68, and 0.54, respectively.

Table 1. Formulations of PEI-EP and DPPEI-EP system

Samples	E51 (g)	PEI (g)	DPPEI (g)
PEI-EP	50.0	21.4	
DPPEI(20)-EP	50.0		12.5
DPPEI(25)-EP	50.0		16.7
DPPEI(30)-EP	50.0		21.4
DPPEI(35)-EP	50.0		27.0

3. Results and Discussion

3.1. Characterization of the DPPEI

To confirm the successful preparation of DPPEI, the chemical structure of the DPPEI was characterized by ^{1}H-NMR and ^{31}P-NMR tests. To clearly illustrate the structure of DPPEI, both PEI and DPPC were also studied The ^{1}H-NMR result is displayed in **Fig. 1**.

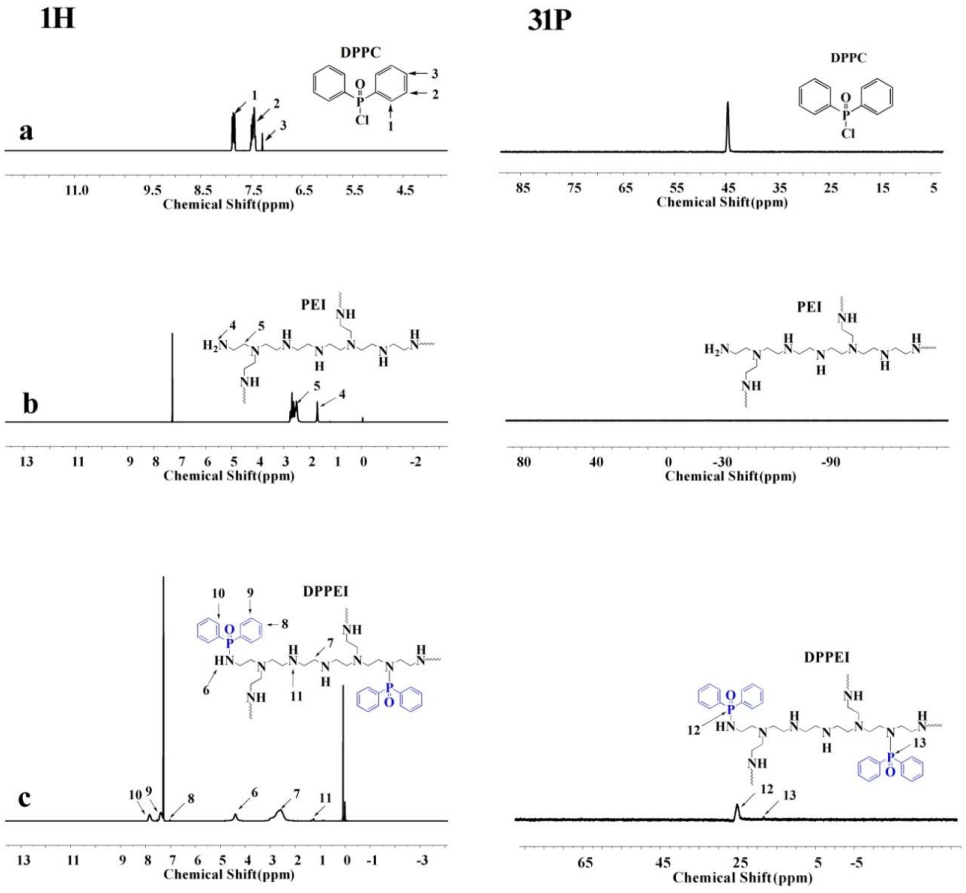

Fig. 1. The ^{1}H-NMR (left column) and ^{31}P-NMR (right column) spectra of DPPC (a), PEI (b), and DPPEI (c).

In **Fig. 1**, the peak at 7.30 ppm is attributed to the -CH- in $CDCl_3$.[32] For DPPEI, it was found that the peak 4 ascribed to the NH_2 group of PEI almost disappeared in its ^{1}H-NMR spectrum. Meanwhile, a new peak (peak 6) appeared at 4.39 ppm in the ^{1}H-NMR spectrum of DPPEI, indicating the formation of -C-NH-P- group. In addition, the peak 8, 9, and 10 in the ^{1}H-NMR spectrum of DPPEI corresponding to the -CH- (peak 3, 2 and 1) of benzene ring in DPPC, peak 7 ($-CH_2-$),[33] and peak 6 (-NH-) existed in the ^{1}H-NMR spectrum of DPPEI. All these results illustrated that the NH_2 group of PEI participated in the reaction between PEI and DPPC, and both PEI and DPPC reacted. The ^{31}P-NMR spectra further demonstrated that the DPPEI with the structure shown in **Fig. 1** was prepared successfully.

In the ^{31}P-NMR spectra, there was only one peak at 44.95 ppm for DPPC, which was from the -P- proton in -P-Cl group. No any typical signal existed in the ^{31}P-NMR spectrum of PEI because of no P in its chemical structure. In comparison with the ^{31}P-NMR result of DPPC and PEI, there were two new characteristic peaks locating at 24.18 and 17.43 ppm for DPPEI, corresponding to the -NH-P- and -N-P-, respectively. This result further verified that the DPPC reacted with the PEI, and the DPPEI with the characteristic structures of -NH-P- and -N-P- was formed. On the basis of the ^{1}H-NMR and ^{31}P-NMR results, it is concluded that the DPPEI with the structure shown in **Scheme 1** was obtained successfully.

3.2. Characterization of the cured DPPEI-EP

XPS measurement was carried out to confirm the crosslinking structure of DPPEI-EP. Here, the DPPEI(30)-EP was chosen as the representative sample in the XPS analysis. Meanwhile, the reference transparent sample PEI-EP was also analyzed through the XPS test for the purpose of comparison. The N_{1s} spectra of DPPEI(30)-EP and PEI-EP are shown in **Fig. 2.** For the PEI-EP, there were three peaks at the binding energies of 399.0 eV, 399.5 eV, and 400.0 eV, corresponding to N～$(C)_3$, (O)～N～$(C)_2$, and (C～)N～$(O)_2$, respectively.[1,34] The peak at 400.0 eV disappeared in the N_{1s} spectra of PEI-EP after the curing reaction of DPPEI-EP, but the other two peaks of PEI-EP still existed in the N_{1s} spectra of PEI-EP. Moreover, two new peaks at 402.1 eV and 402.4 eV appeared for DPPEI(30)-EP. The two new peaks are ascribed to the $(C)_2$～N-P- and (O)(C)～N-P- groups, respectively,[22,34] indicating that epoxy group was opened by the amine group of DPPEI. According to the XPS result, the curing process can be concluded as follows. At a certain temperature, the epoxy group was opened by the amine group, which resulted in the generation of a hydroxyl

group and more secondary/tertiary amine. The newly formed hydroxyl group further reacted with another epoxy group.[1] Therefore, a crosslinking network with both amine group and ether linkages was obtained in DPPEI(30)-EP. The curing process is shown in **Scheme 2**.

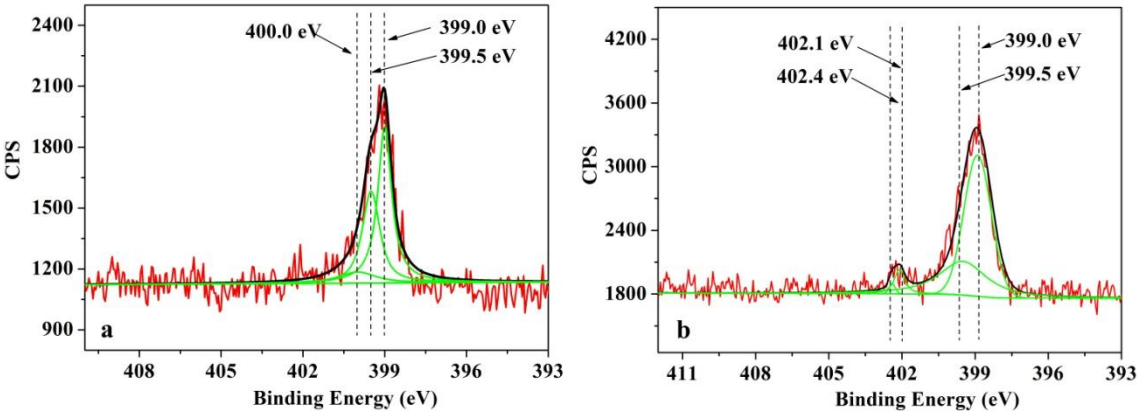

Fig.2. N_{1s} spectra of the PEI-EP (a) and DPPEI-EP (b).

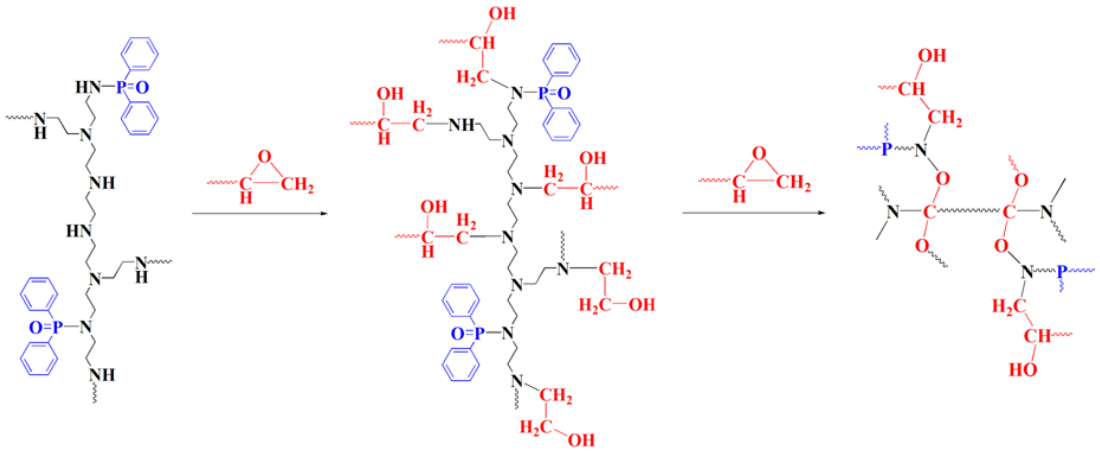

Scheme 2. Curing process of the DPPEI-EP.

Generally, the crosslinking density is an important parameter for the cured EP. To illustrate the crosslinking behavior, the DMA test was performed, and the result is shown in **Fig. 3** and **Table 2**. To be quantitative, using the following equation [35]:

$$E_r = 3RT_r\upsilon_e$$

Here, the R is the universal gas constant (8.314 J/K.mol), the T_r corresponding to E_r is the temperature taken as 30 °C above the glass transition temperature (T_g), and the υ_e is the crosslinking density.

First, the T_g values of these cured EPs were measured. As shown in **Fig. 3**, the T_g values of PEI-EP, DPPEI(20)-EP, DPPEI(25)-EP, DPPEI(30)-EP and DPPEI(35)-EP were 43.5 °C, 52.8 °C, 56.1 °C, 50.1 °C, and 47.3 °C, respectively. Obviously, the DPPEI-EP system has higher T_g than PEI-EP in the DPPEI range from 20 wt% to 35 wt%. Moreover, the T_g of DPPEI-EP first increased and then decreased with increasing the content of DPPEI, which must be related to the change of thermo-setting network and crosslinking density. [36-37] The calculated crosslinking densities are listed in **Table 2**. For PEI-EP, the crosslinking density was 3420 mol/m^3. Here, the content of PEI was 30 wt%. After incorporation of the DPPEI from 20 wt% to 35 wt%, the crosslinking density first increased from 2289 mol/m^3 to 2997 mol/m^3, then decreased to 2391 mol/m^3. Obviously, the change of crosslinking density has the same trend as that of T_g.

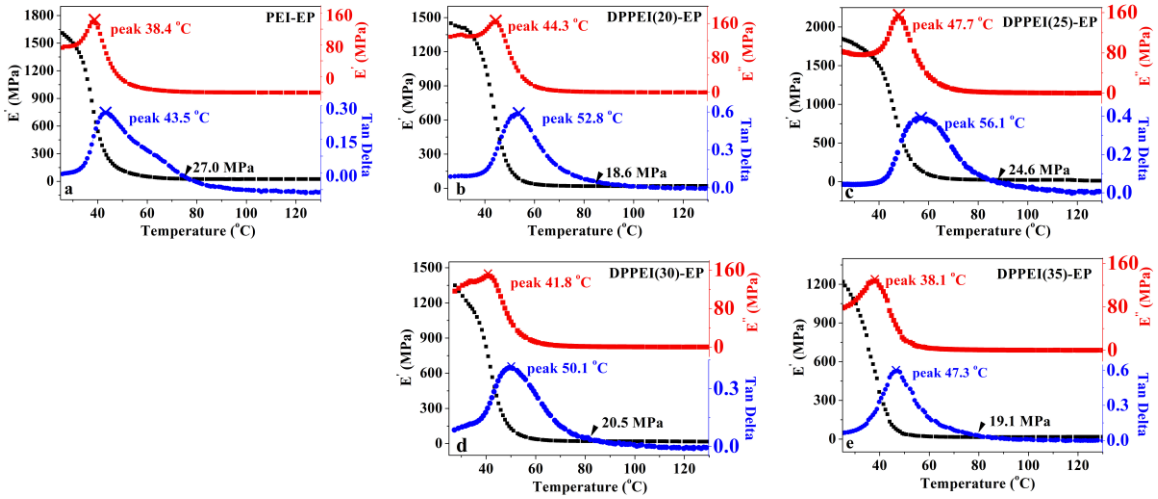

Fig. 3. The storage moduli (E'), loss moduli (E'') and tan σ of the cured PEI-EP (a), DPPEI(20)-EP (b), DPPEI(25)-EP (c), DPPEI(30)-EP (d), and DPPEI(35)-EP (e) in DMA test.

Table 2. Glass transition temperatures, storage moduli and crosslink densities of the cured EPs

	PEI-EP	DPPEI (20)-EP	DPPEI (25)-EP	DPPEI (30)-EP	DPPEI (35)-EP
T_g (°C)	43.5	52.8	56.1	50.1	47.3
Storage modulus (Er, MPa)	27.0	18.6	24.6	20.5	19.1
Crosslinking density (υ_e, mol/m^3)	3420	2289	2997	2544	2391

In addition, the content of chlorine (Cl) is very important for the application of DPPEI-EP, so it is necessary to confirm whether there was the residual Cl after the curing process or not. Here, the DPPEI(30)-EP was chosed as the representative sample. The XPS result of DPPEI(30)-EP is shown in **Fig. 4**. Generally, the accuracy of XPS is about 0.01 wt%. According to the XPS result shown in **Fig. 4**, the DPPEI-EP contained the carbon (C), nitrogen (N), oxygen (O), and phosphorus (P), but there was no Cl. The XPS result illustrated that no Cl was left in the DPPEI-EP, or the content of chlorine was lower than 0.01 wt% in the DPPEI-EP, suggesting that the effect of left Cl on the cured DPPEI-EP should not be considered. In addition, the contents of the P in DPPEI-EPs were investigated through ICP-AES, and the result is shown in **Table 3**. Contents of the P for DPPEI(20)-EP, DPPEI(25)-EP, DPPEI(30)-EP, and DPPEI(35)-EP were 1.13 wt%, 1.35 wt%, 1.65 wt%, and 1.99 wt%, respectively, which are close to the corresponding theoretical value. Here, the theoretical value of P was calculated on the basis of the weight ratio of DPPEI/EP. This result further illustrated that the cured DPPEI-EPs with the structure shown in **Scheme 2**

were prepared successfully.

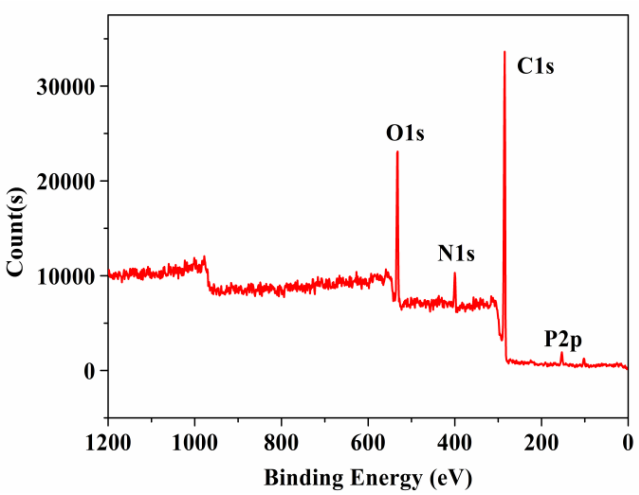

Fig. 4. XPS result of the DPPEI(30)-EP

Table 3. ICP-AES data of the DPPEI-EPs

	DPPEI	DPPEI(20)-EP	DPPEI(25)-EP	DPPEI(30)-EP	DPPEI(35)-EP
P (wt%)	5.82	1.13	1.35	1.65	1.99
Theoretical P (wt%)	6.00	1.20	1.50	1.80	2.10

Next, the dispersion of DPPEI in DPPEI-EP was investigated through SEM-EDX. For the DPPEI-EP, the typical elemental difference in comparison with the uncured EP is the P. Obviously, the distribution of P represents the dispersion of the DPPEI in the cured DPPEI-EP. **Fig. 5** shows that the ditribution of P in the cured DPPEI-EP is quite homogeneous, illustrating that the DPPEI was well distributed in EP after a curing process. Here, it should be noted that these yellow points represent the existence of P in **Fig. 5b**.

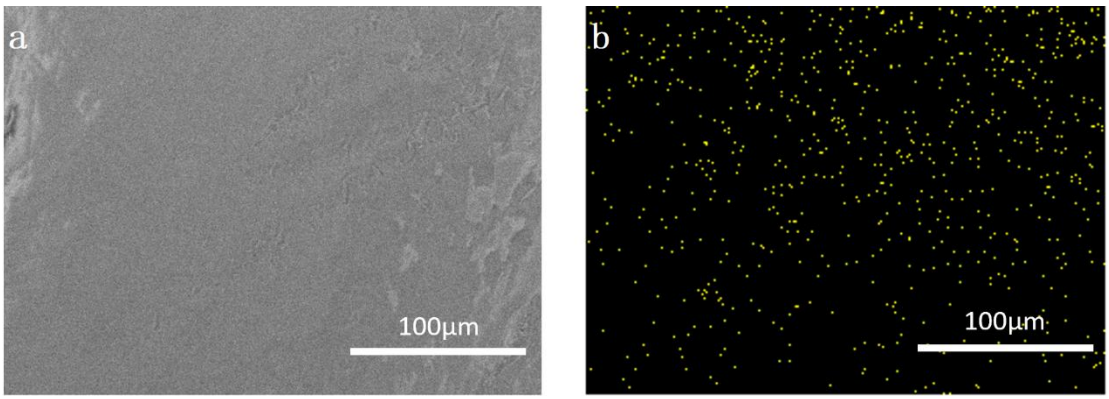

Fig. 5. SEM micrograph (a) of DPPEI(30)-EP and its corresponding EDX micrograph (b).

3.3. Transparency of the cured DPPEI-EP

Fig. 6 shows the transparency of PEI-EP and DPPEI-EPs samples with the thickness of 1.0 mm. All these words can be clearly seen through five samples, illustrating that the PEI-EP and all the DPPEI-EPs had good transparency in the visible region. To quantitatively verify that the DPPEI had no influence on the transparency of cured EP, the transmittances of PEI-EP and DPPEI-EPs were investigated. Within the wavelength range measured, the DPPEI-EPs showed broad transmission spectra. **Fig. 7** shows that the transmittance of reference transparent sample PEI-EP is almost equal to that of DPPEI-EP. With increasing the content of P in the cured EP, the transmittance of the cured DPPEI-EP was scarcely affected, and kept at about 90% in the visible region. Generally, the inner structure of materials plays an important role in determining their optical transmittance. The polymer with completely amorphous structure has a high optical transmittance In addition, The polymer materials with low crystallinity and small size of crystals also have a high optical transmittance because the scattering of light is also small at grain boundaries when a beam of light travels from one grain to another one. For most of flame-retarded EP materials, there are some grains through which the scattering of light is strong, so these flame-retarded EPs

are opaque.

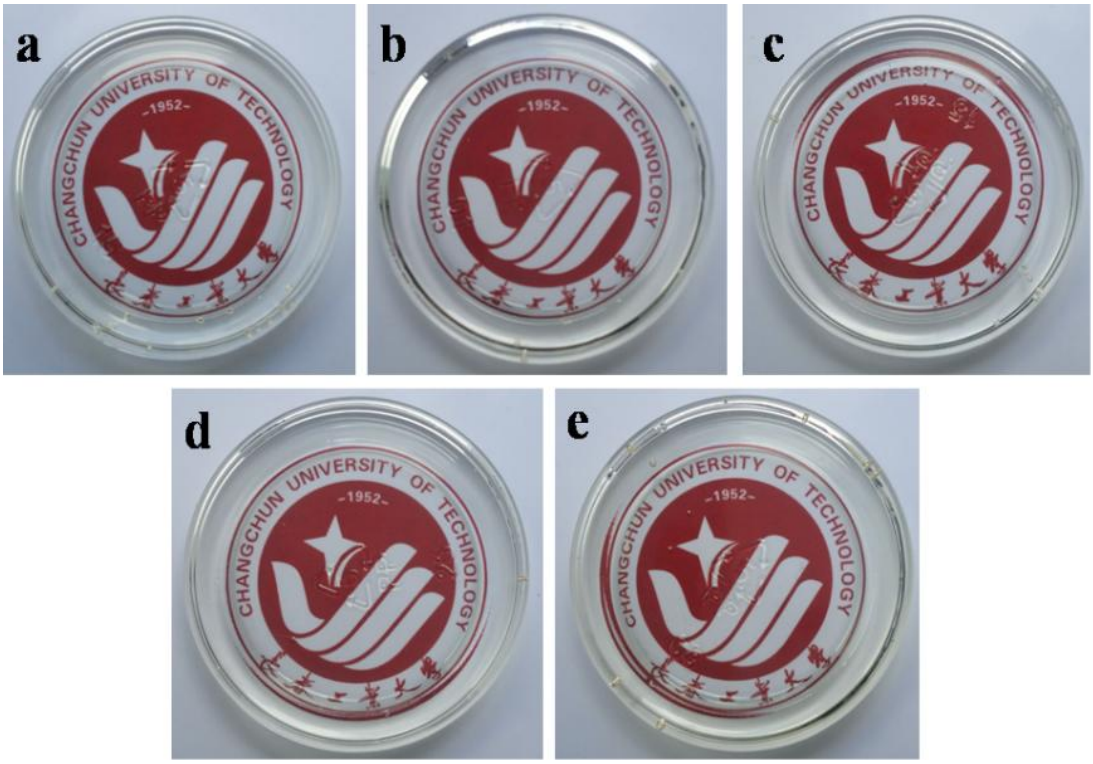

Fig. 6. Digital photos of the cured EPs: a, PEI-EP; b, DPPEI(20)-EP; c, DPPEI(25)-EP; d, DPPEI(30)-EP; e, DPPEI(35)-EP.

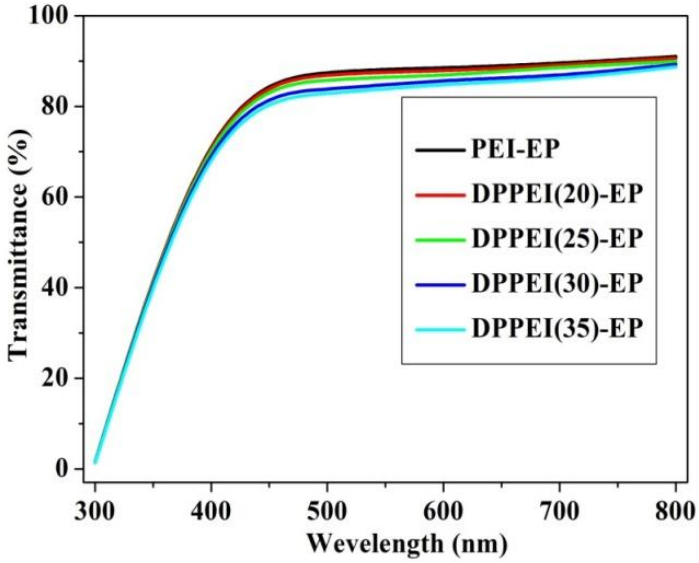

Fig. 7. Transmittances of the cured DPPEI-EPs and reference sample PEI-EP.

Fig. 8 shows the XRD patterns of DPPEI-EPs and the reference transparent sample PEI-EP. There was only one background peak for all samples in the 2θ range from 5^{o} to 45^{o},

illustrating that the inner structure of all samples were amorphous. According to the above analysis, it is known that this kind of amorphous inner structure contributed to the transparency of DPPEI-EPs. Obviously, the excellent transparency of DPPEI-EPs should be ascribed to its amorphous condensed phase.

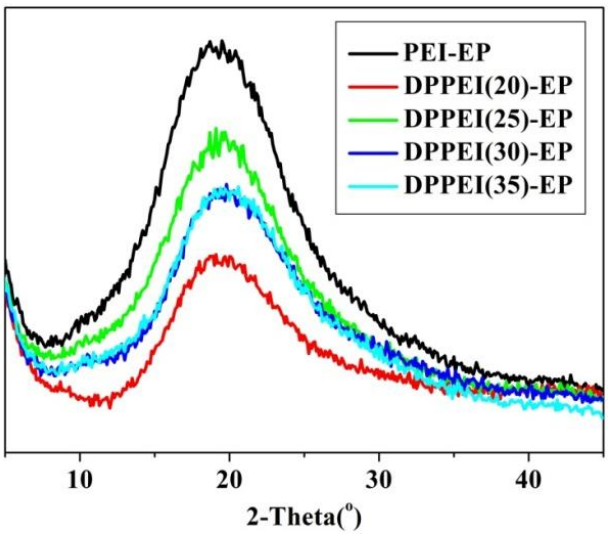

Fig. 8. XRD paterns of PEI-EP and DPPEI-EPs.

3.4. Mechanical properties of the cured EP

Mechanical properties of the cured EPs, including tensile strength, elongation at break, and impact strength, are listed in **Table 4.** The mechanical properties of DPPEI(20)-EP are apparently worse than those of DPPEI-EP with higher content (25～35 wt%) of DPPEI. With increasing the content of DPPEI from 25 to 35 wt%, the tensile strength, flexural strength, and impact strength of cured DPPEI-EP have no great change. At equal amount of curing agent PEI and DPPEI, there is also no obvious change in tensile strength, flexural strength, and impact strength between PEI-EP and DPPEI(30)-EP. Obviously, the DPPEI did not deteriorate the mechanical properties of cured EP compared with the PEI.

Table 4. Mechanical properties of the cured EP

Sample	Tensile strength (MPa)	Flexural strength (MPa)	Impact strength (kJ/m^2)
PEI-EP	52.6±2.3	89.8±3.8	7.5±0.4
DPPEI(20)-EP	48.4±3.5	70.3±1.9	6.1±0.2
DPPEI(25)-EP	51.4±3.5	82.3±2.3	6.9±0.3
DPPEI(30)-EP	51.5±1.7	88.9±2.4	7.4±0.5
DPPEI(35)-EP	53.4±3.7	84.6±4.5	7.0±0.7

The possible reason for no obvious change in mechanical properties with increasing the DPPEI may be explained as follows. First, it is known that the chemical linkages of the thermo-setting networks are the key factors. According to the calculation result shown in the **Table 2**, it is known that the crosslinking density of cured DPPEI-EP first increased, and then decreased. Theoretically, the strength of cured epoxy is dominated by the crosslinking density if there is only one changeless network in the cured EP. However, for the DPPEI, there were three kinds of amino groups. When the amount of the DPPEI was low, three kinds of amino groups might participate in the curing reaction. With increasing the DPPEI, the amount of primary amine which participated in the curing reaction might gradually increase. Moreover, more and more hydrogen bonding might be formed with continuously increasing the DPPEI. On the basis of the above reasons, the thermo-setting networks of DPPEI-EP must be gradually changed with increasing the content of DPPEI, so the mechanical properties of cured DPPEI-EP might be not apparently affected when the crosslinking density changed with increasing the content of DPPEI. In this work, the change of

thermo-setting networks must be the leading reason why the mechanical properties of DPPEI-EP were not apparently affected with increasing the DPPEI.

3.5. Flame retardancy of the cured EP

The flame retardancy of the cured EP was evaluated by the LOI and UL-94 tests, and the corresponding results are shown in **Table 5**. The reference sample PEI-EP had the LOI value of 18.3%, and did not pass the UL-94 V-0 rating (3.2 mm). However, the LOI value of DPPEI-EP increased significantly compared with that of PEI-EP, and continued going up with increasing the DPPEI. When the DPPEI content was 30 wt%, the LOI value of DPPEI-EP increased to 27.7%. Moreover, the cured DPPEI-EP passed the UL-94 V-0 rating (3.2 mm), and no dripping was observed. Further increasing the DPPEI to 35 wt%, the LOI of DPPEI(35)-EP reached 29.8%. Meanwhile, the DPPEI(35)-EP with the thickness of 1.6 mm passed the UL-94 V-0 rating, and had no dripping during burning. Obviously, the thin and transparent DPPEI-EP sample has excellent flame retardancy, which may further promote the potential application value of DPPEI-EP.

Table 5. LOI and UL-94 results of the cured DPPEI-EPs and reference sample PEI-EP.

Sample	LOI	UL-94 (3.2 mm)		UL-94 (1.6 mm)	
	(%)	Rating (t_1+t_2)	Dripping	Rating (t_1+t_2)	Dripping
PEI-EP	18.3	NR (>50 s)	Yes	NR (>50 s)	Yes
DPPEI(20)-EP	21.5	V-2 (40～50 s)	Yes	NR (>50 s)	Yes
DPPEI(25)-EP	25.1	V-1 (20～30 s)	No	NR (>50 s)	Yes
DPPEI(30)-EP	27.7	V-0 (2～5 s)	No	V-1 (15-25 s)	No
DPPEI(35)-EP	29.8	V-0 (1～3 s)	No	V-0 (1-5 s)	No

The CC test was used to illustrate the combustion behavior of the cured EP, and the corresponding result is shown in **Fig. 9** and **Table 6**. Here, the DPPEI(30)-EP was chosen as the representative sample because of its excellent flame retardancy in the UL-94 and LOI tests. The peak of heat release rate (PHRR) of reference sample PEI-EP was 1770 kW/m^2, and its total heat release (THR) was 98.5 MJ/m^2. After incorporation of 30 wt% DPPEI into the EP, the PHRR and THR of DPPEI(30)-EP greatly decreased to 645 kW/m^2 and 30.0 MJ/m^2, respectively, and correspondingly reduced by 63.6% and 69.5%. Based on the HRR curves, the FGR was calculated to assess the fire hazard of the DPPEI(30)-EP according to the following equation:[38-39]

$$FGR = PHRR/t_{PHRR}$$

Generally, a lower FGR value indicates that the time to flashover is delayed, which allows enough time to evacuate in distress and/or arrive for fire extinguishers.[40] Compared with the FGR of PEI-EP, the value of DPPEI(30)-EP decreased to 8.4 kW/m^2.s from 15.4 kW/m^2.s, illustrating that the DPPEI(30)-EP had better fire safety than PEI-EP.

Smoke produced during burning may lead to people's death by suffocation and/or inhalation of the toxic gases, thus, the estimation for smoke suppression is very important for flame-retarded polymers. The smoke production rate (SPR) and total smoke production (TSP) plots as a function of time for DPPEI(30)-EP and reference sample PEI-EP are presented in **Fig. 9**, and the corresponding data are shown in **Table 6**. The SPR of DPPEI(30)-EP reduced to 0.565 m^2/s from 1.253 m^2/s of PEI-EP. Moreover, the TSP value of DPPEI(30)-EP decreased to 31.6 m^2, much lower than that of PEI-EP. These results illustrated that the DPPEI efficiently restrained the production of smoke of cured EP during burning.

According to these results presented above, it is concluded that the synthesized DPPEI endowed the cured EP with simultaneous excellent transparency and flame retardancy.

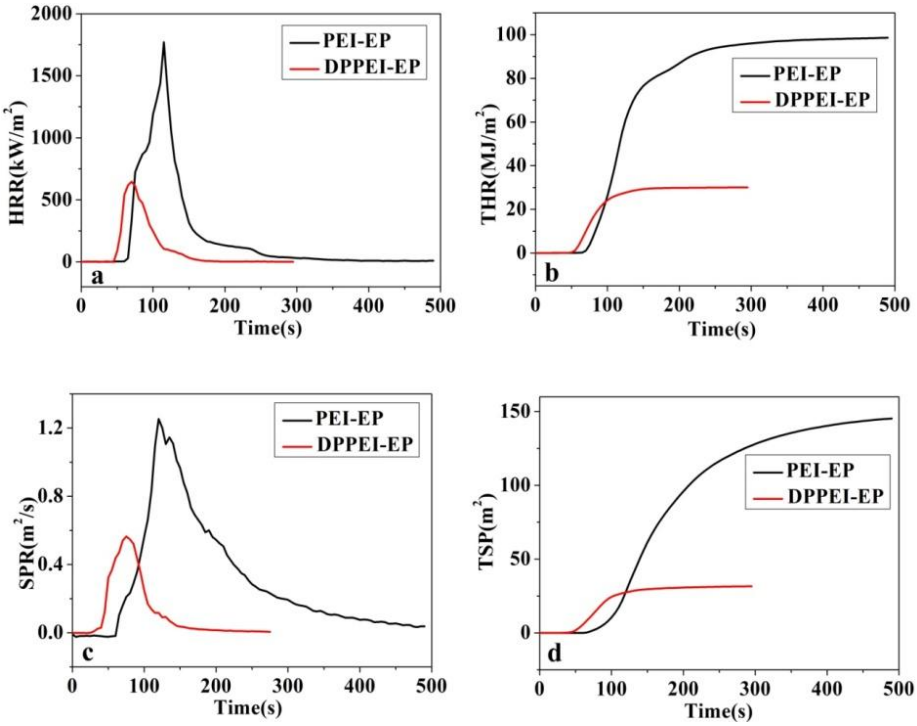

Fig. 9. HRR (a), THR (b), SPR (c), and TSP (d) plots of PEI-EP and DPPEI(30)-EP.

Table 6. CC data of DPPEI(30)-EP and reference sample PEI-EP

Sample	PEI-EP	DPPEI-EP
TTI (s)	58	47
Peak HRR (kW/m^2)	1770	645
Time to PHRR (s)	115	77
FGR (kW/m^2.s)	15.4	8.4
THR (MJ/m^2)	98.5	30.0
Peak SPR (m^2/s)	1.253	0.565
TSP (m^2)	145.3	31.6
Residue (%)	3.2	15.0

3.6. Flame-retardant mechanism of DPPEI-EP

To reveal the flame-retardant mechanism of DPPEI-EP, the residue of DPPEI(30)-EP after CC test was firstly investigated through digital photos. **Fig. 10** shows that there was small amount of residue after the burning process for the reference sample PEI-EP, while much more residue was obtained for the DPPEI(30)-EP. Moreover, the residue of DPPEI(30)-EP was compact and continuous. Generally, a compact char layer may effectively provide a barrier between fire and materials underneath and protect the underlying materials. Here, the good flame retardancy of DPPEI(30)-EP should be related to the formation of a compact and continuous char layer.

Fig. 10. Digital photographs of the residues of PEI-EP (a) and DPPEI(30)-EP (b).

To further support the above viewpoint, the residues of DPPEI(30)-EP and PEI-EP were analyzed through FTIR, and the result is shown in **Fig. 11**. Compared with the residue of PEI-EP, the peaks corresponding to P-O-C appeared at around 1129.7 cm^{-1} and 914.6 cm^{-1} for the residue of DPPEI(30)-EP.[41] Meanwhile, a new peak was observed at about 715.8 cm^{-1}, indicating the formation of P-N-C.[42] These structures from the thermal decomposition of DPPEI were deposited in the residue, which were very important for the stabilization and

compactness of the residue of DPPEI(30)-EP.[43] However, these structures did not exist in the residue of the reference sample PEI-EP, meaning that the structural difference of residues must be an important reason for the different flame retardancy between DPPEI(30)-EP and PEI-EP.

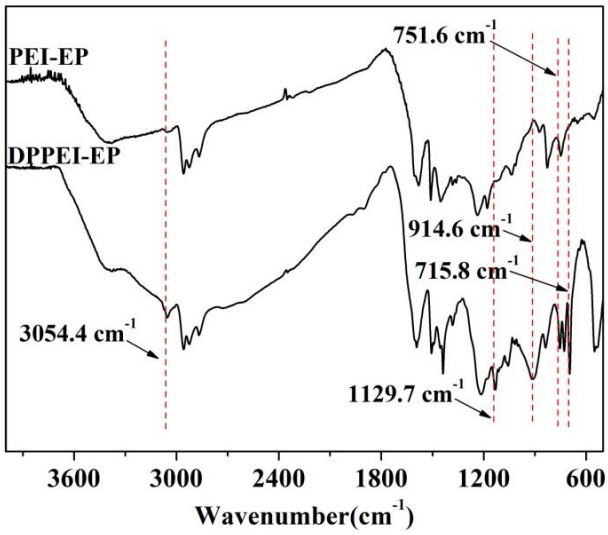

Fig. 11. FTIR spectra of the condensed products of PEI-EP and DPPEI(30)-EP.

In order to further confirm the effect of the formed condensed phase of DPPEI(30)-EP on its flame retardancy, the XPS test was used to analyze the residue. The contents of C, N, O, and P are displayed in **Table 7**. For the residue of DPPEI(30)-EP, the content of P was 4.3 wt%, higher than that of PEI-EP; the contents of N and O were 10.4 wt% and 15.6 wt%, respectively, also higher than the corresponding value of PEI-EP. Combined with the FTIR result, it is known that the higher contents of P, N, and O in the residue of DPPEI(30)-EP should be ascribed to the formation of P-O-C, P-N-C, etc. structures, indirectly proving that the condensed mechanism played an important role in the flame retardancy of DPPEI(30)-EP.

Table 7. XPS data of the condensed products of PEI-EP and DPPEI-EP after CC test

Sample	C (wt%)	N (wt%)	P (wt%)	O (wt%)
PEI-EP	74.0	10.4	0.0	15.6
DPPEI-EP	60.7	17.7	4.3	17.3

In order to further study the effect of DPPEI on the flame retardancy of EP, the gaseous phases of PEI and DPPEI were also investigated through TG-FTIR. **Fig. 12** shows the TG result. For PEI and DPPEI, there were two decomposing processes. For the PEI, the corresponding T_{max} (the temperature at the maximum decomposing rate) values were 358.7 °C and 395.7 °C. However, the corresponding T_{max} of DPPEI shifted to a lower value. In addition, the mass loss rate of DPPEI was slower than that of PEI. According to the TG result, the thermal decomposing behavior of DPPEI is different from that of PEI, which should be due to the incorporation of P-N with the benzene ring into PEI. The FTIR spectra of the gaseous phases of PEI and DPPEI during the thermal decomposition process are shown in **Fig. 13**. The absorbing peaks of ammonia (NH_3) at 928.8 cm^{-1} and 964.1 cm^{-1} appeared at 292 °C for the PEI,[44] and still existed before 416 °C. The peaks at 2944.1 and 2812.2 cm^{-1} are ascribed to the C-H.[12,45-46] However, for the DPPEI, the absorbing peaks of C-H at 2947.6 cm^{-1} and 2824.3 cm^{-1} began to appear at 272 °C, and the absorbing peaks of NH_3 also appeared at 929.3 cm^{-1} and 963.5 cm^{-1} under this temperature, indicating that the DPPEI had the earlier release of NH_3 than the PEI. For the DPPEI, two new peaks corresponding to the C-H in benzene ring appeared at 3066.1 cm^{-1} and 2878.3 cm^{-1} at about 388°C. Meanwhile, another two new peaks locating at 1171.0 cm^{-1} and 700.5 cm^{-1} also appeared at this temperature, corresponding to the P-O and P-C,[12,45-46] which indicated that

the P-O and P-C structures with the benzene ring were formed in the gaseous products during the thermal decomposition of DPPEI.[47] In addition, some other gaseous sections were also produced, including P=O (1259.2 cm^{-1}), C-C of aromatic ring (1607.2 cm^{-1}, 1510.4 cm^{-1}, and 1460.0 cm^{-1}), P-Ph (1460 cm^{-1}), etc. Obviously, the gaseous products containing P contributed to the gas-phase flame retardance of DPPEI-EP.[12, 46]

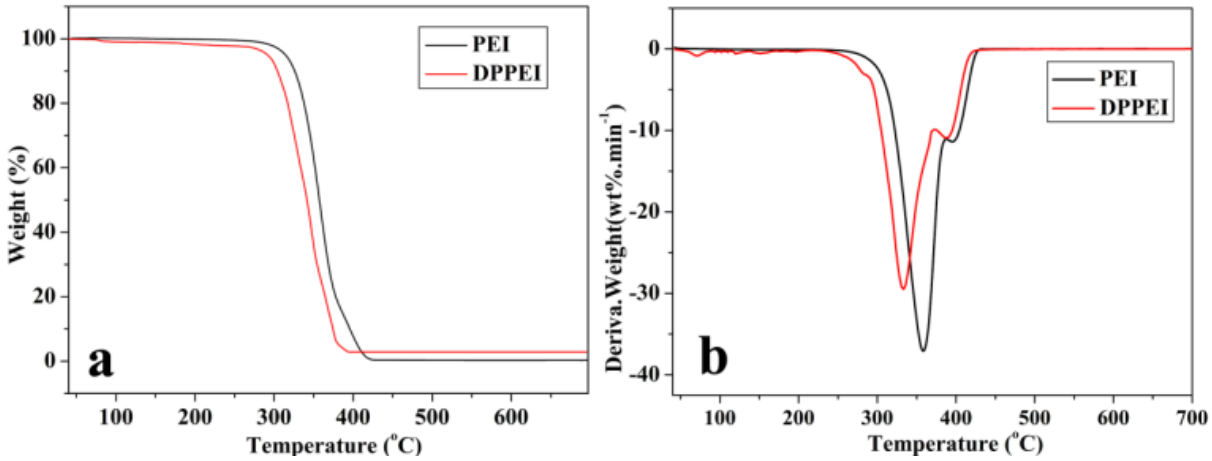

Fig. 12. TG (a)and DTG (b) curves of PEI and DPPEI under N_2 atmosphere.

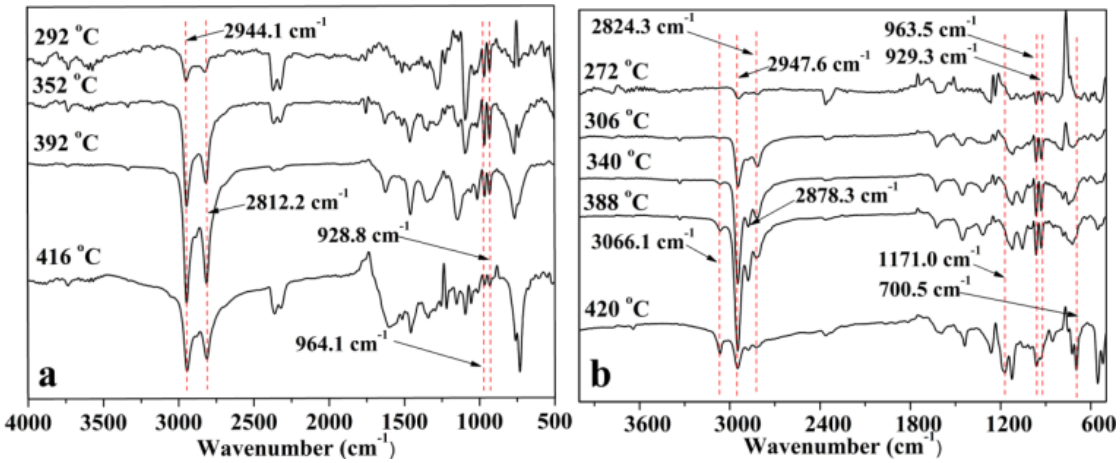

Fig. 13. FTIR spectra of the gaseous products of PEI (a) and DPPEI (b).

According to the FTIR, XPS, and TG results, the possible flame-retardant mechanism of DPPEI-EP during the combustion process is concluded as follows. As shown in **Scheme 3**, the NH_3, P-C with benzene ring, etc, were first formed during the thermally decomposing process of DPPEI-EP. These gaseous products played their roles through diluting the

combustible gases. Meanwhile, the residue consisting of P-O-C, P-N-C, etc. was formed during the combustion process, resulting in the formation of a stable and compact char layer which might act as a barrier between the burning zone and the material underneath. Obviously, both gas phase and condensed phase simultaneously acted during the combustion process and led to the significant improvement of flame retardancy of DPPEI-EP compared with that of PEI-EP.

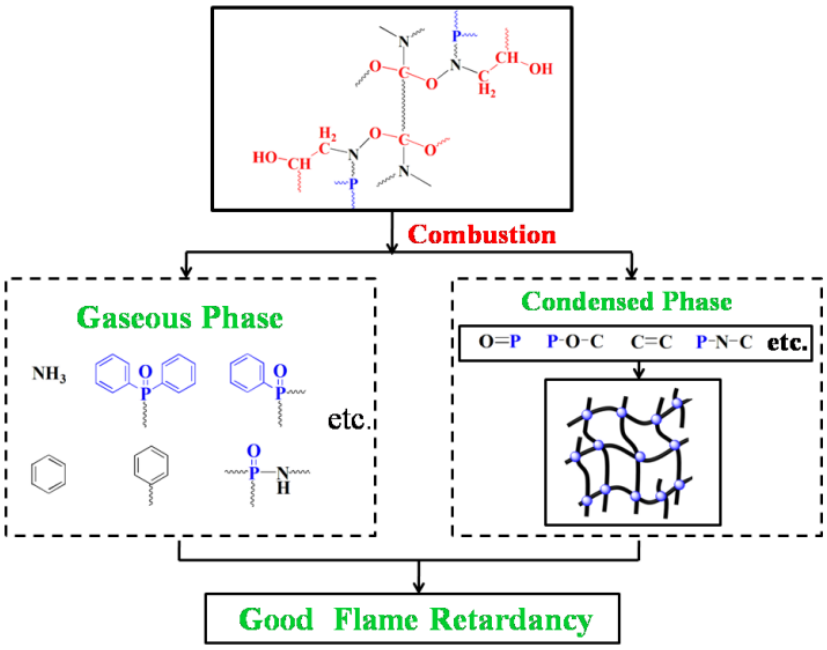

Scheme 3. Flame-retardant mechanism of DPPEI-EP during the combustion process.

4. Conclusion

A novel polymeric curing agent DPPEI was prepared successfully in this work. The amine group in DPPEI participated in the curing reaction of EP and then endowed the EP with simultaneous transparency and flame retardancy. The cured DPPEI-EP achieved the V-0 rating (1.6 mm) and the LOI of 29.5%, meanwhile, the transmittance of DPPEI-EP kept at a high level of about 90% in the visible region. During burning, the DPPEI-EP presented low heat release and low smoke release, much lower than the corresponding value of transparent

reference sample PEI-EP. Obviously, the synthesized curing agent DPPEI was an efficient polymeric curing agent in preparing the EP with simultaneous flame retardancy and transparency, so it has great potential application value in gradient coating, light-emitting diodes (LEDs), arts, etc. fields.

Acknowledgment

This work was support by the National Natural Science Foundation of China (grant number 51703011); Project of Jilin Provincial Department of Education (grant no. 2016329) and Program of Jilin Provincial Department of Science & Technology (grant no. 20170520125JH).

References

(1) Tan, Y.; Shao, Z. B.; Yu, L. X.; Long, J. W.; Qi, M.; Chen, L. and Wang, Y. Z. Piperazine-modified ammonium polyphosphate as monocomponent flame-retardant hardener for epoxy resin: flame retardance, curing behavior and mechanical property. *Polym. Chem.* **2016**, *7*, 3003-3012.

(2) Jiang, S. D.; Bai, Z. M.; Tang, G.; Song, L.; Stec, A. A.; Hull, T. R.; Hu, Y. and Hu, W. Z. Synthesis of Mesoporous Silica@Co–Al Layered Double Hydroxide Spheres: Layer-by-Layer Method and Their Effects on the Flame Retardancy of Epoxy Resin. *ACS Appl. Mater. Interfaces* **2014**, *6*, 14076-14086.

(3) Zhang, X.; He, Q.; Gu, H.; Colorado, H. A.; Wei, S. and Guo, Z. Flame-Retardant Electrical Conductive Nanopolymers Based on Bisphenol F Epoxy Resin Reinforced with Nano Polyanilines. *ACS Appl. Mater. Interfaces* **2013**, *5*, 898-910.

(4) Jiang, J.; Cheng, Y. B.; Liu, Y.; Wang, Q.; He, Y. S. and Wang, B. W. Intergrowth charring for flame-retardant glass fabric-reinforced epoxy resin composites. *J. Mater. Chem. A* **2015**, *3*, 4284-4290.

(5) Qian, L. J.; Qiu, Y.; Wang, J. Y. and Xi, W. High-performance flame retardancy by char-cage hindering and free radical quenching effects in epoxy thermosets. *Polymer* **2015**, *68*, 262-269.

(6) Jian, X. Y.; He, Y.; Li, Y. D.; Wang, M.; Zeng, J. B. Curing of epoxidized soybean oil with crystalline oligomeric poly(butylene succinate) towards high performance and sustainable epoxy resins. *Chem. Eng. J.* **2017**, *326*, 875-885.

(7) Ma, C.; Qiu, S. L.; Yu, B.; Wang, J. L.; Wang, C. M.; Zeng, W. R.; Hu, Y. Economical and environment-friendly synthesis of a novel hyperbranched poly(aminomethylphosphine oxide-amine) as co-curing agent for simultaneous improvement of fire safety, glass transition temperature and toughness of epoxy resins. *Chem. Eng. J.* **2017**, *322*, 618-631.

(8) Huang, Y. W.; Song, S. Q.; Yang, Y.; Cao, K.; Yang, J. X. and Chang, G. J. Decomposable double-walled hybrid nanorods: formation mechanism and their effect on flame retardancy of epoxy resin composites. *J. Mater. Chem. A* **2015**, *3*, 15935-15943.

(9) Kalali, E. N.; Wang, X. and Wang, D. Y. Functionalized layered double hydroxide-based epoxy nanocomposites with improved flame retardancy and mechanical properties. *J. Mater. Chem. A* **2015**, *3*, 6819-6826.

(10) Shi, Y. Q.; Yu, B.; Zheng, Y. Y.; Guo, J.; Chen, B. H.; Pan, Z. M.; Hu Y. A combination of POSS and polyphosphazene for reducing fire hazardsof epoxy resin. *Polym. Adv. Technol.* **2017**, DOI: 10.1002/pat.4235.

(11) Qiu, S. L.; Shi, Y. Q.; Wang, B. B.; Zhou, X.; Wang, J. L.; Wang, C. M.; Gangireddy, C. S. R.; Yuen, K. K. R.; Hu, Y. Constructing 3D Polyphosphazene Nanotube@Mesoporous Silica@Bimetallic Phosphide Ternary Nanostructures via Layer-by-Layer Method: Synthesis and Applications. *ACS Appl. Mater. Interfaces* **2017**, *9*, 23027-23038.

(12) Yu. B.; Shi, Y. Q.; Yuan, B. H.; Qiu, S. L.; Xing, W. Y.; Hu, W. Z.; Song, L.; Lo, Siuming, Hu. Y. Enhanced thermal and flame retardant properties of flame-retardant-wrappedgraphene/epoxy resin nanocomposites. *J. Mater. Chem. A* **2015**, *3*, 8034-8044.

(13) Kong, Q. H.; Wu, T.; Zhang, J. H.; Wang, D. Y. Simultaneously improving flame retardancy and dynamic mechanical properties of epoxy resin nanocomposites through layered copper phenylphosphate. *Compos. Sci. Technol.* **2018**, *154*, 136-144.

(14) Gu, J. W.; Liang, C. B.; Zhao, X. M.; Gan, B.; Qiu, H.; Guo, Y. Q.; Yang, X. T.; Zhang, Q. Y.; Wang, D. Y. Highly thermally conductive flame-retardant epoxy nanocomposites with reduced ignitability and excellent electrical conductivities. *Compos. Sci. Technol.* **2017**, *139*, 83-89.

(15) Luo, Q. Q.; Yuan, Y. C.; Dong, C. L.; Liu, S. M. and Zhao, J. Q. Intumescent flame retardancy of a DGEBA epoxy resin based on 5,10-dihydro-phenophosphazine-10-oxide. *RSC Adv*. **2015**, *5*, 68476-68484.

(16) Wang, J. S.; Wang, D. Y.; Liu, Y.; Ge, X. G.; Wang, Y. Z. Polyamide-enhanced flame retardancy of ammonium polyphosphate on epoxy resin. *J. Appl. Polym. Sci.* **2008**, *108*, 2644-2653.

(17) Jiao, C. M.; Zhang, C. J.; Dong, J.; Chen, X. L.; Qian, Y. and Li, S. X. Combustion

behavior and thermal pyrolysis kinetics of flame-retardant epoxy composites based on organic-inorganic intumescent flame retardant. *J. Therm. Anal. Calorim.* **2015**, *119*, 1759-1767.

(18) Zhou, X.; Qiu, S. L.; Xing, W. Y.; Gangireddy, C. S. R.; Gui, Z.; Hu, Y. Hierarchical Polyphosphazene@Molybdenum Disulfide Hybrid Structure for Enhancing the Flame Retardancy and Mechanical Property of Epoxy Resins. *ACS Appl. Mater. Interfaces* **2017**, *9*, 29147-29156.

(19) Hou, Y. B.; Hu, W. Z.; Gui, Z.; Hu, Y.A novel Co(Ⅱ)–based metal-organic framework with phosphorus-containing structure: Build for enhancing fire safety of epoxy. *Compos. Sci. Technol.* **2017**, *152*, 231-242.

(20) Yang, S.; Zhang, Q. X.; Hu, Y. F. Synthesis of a novel flame retardant containing phosphorus, nitrogen and boron and its application in flame-retardant epoxy resin. *Polym. Degrad. Stab.* **2016**, *133*, 358-366.

(21) Rajaei, M.; Wang, D. Y.; Bhattacharyya, D. Combined effects of ammonium polyphosphate and talc on the fire and mechanical properties of epoxy/glass fabric composites. *Compos. Part B: Eng.* **2017**, *113*, 381-390.

(22) Tan, Y.; Shao, Z. B.; Chen, X. F.; Long, J. W.; Chen, L. and Wang, Y. Z. A Novel Multifunctional Organic-Inorganic Hybrid Curing Agent with High Flame-Retardant Efficiency for Epoxy Resin. *ACS Appl. Mater. Interfaces* **2015**, *7*, 17919-17928.

(23) Liang, B.; Cao, J.; Hong, X. D. and Wang, C. S. Synthesis and properties of a novel phosphorous- containing flame- retardant hardener for epoxy resin. *J. Appl. Polym. Sci.* **2013**, *128*, 2759-2765.

(24) Gu, J. W.; Dang, J.; Wu, Y. L.; Xie, C. and Han, Y. Flame-retardant, thermal, mechanical and dielectric properties of structural non-halogenated epoxy resin composite. *Polym. Plast. Technol. Eng.* **2012**, *51*, 1198-1203.

(25) Hu, J. H.; Shan, J. Y.; Wen, D. H.; Liu, X. X.; Zhao, J. Q. and Tong, Z. Flame retardant, mechanical properties and curing kinetics of DOPO-based epoxy resin. *Polym. Degrad. Stab.***2014**, *109*, 218-225.

(26) Shieh, J. Y. and Wang, C. S. Synthesis of novel flame retardant epoxy hardeners and properties of cured product. *Polymer* **2001**, *42*, 7617-7625.

(27) Wang, C. S. and Shieh, J. Y. Synthesis and properties of epoxy resins containing 2-(6-oxid-6H-dibenz[c,e][1,2]oxaphosphorin-6-yl)1, 4-benzenediol. *Polymer* **1998**, *39*, 5819-5826.

(28) Li, Y. Q.; Fu, S. Y.; Mai, Y, W. Preparation and characterization of transparent ZnO/epoxy nanocomposites with high-UV shielding efficiency. *Polymer* **2006**, *47*, 2127-2132.

(29) Li, Y. Q.; Yang, Y.; Fu, S. Y. Photo-stabilization properties of transparent inorganic UV-filter/epoxy nanocomposites. *Compos. Sci. Technol.* **2007**, *67*, 3465-3471.

(30) Lin, C. H.; Chou, Y. C.; Shiao, W. F.; Wang, M. W. High temperature, flame-retardant, and transparent epoxy thermosets prepared from an acetovanillone-based hydroxyl poly(ether sulfone) and commercial epoxy resins. *Polymer* **2016**, *97*, 300-308.

(31) Luo, C. Y.; Zuo, J. D.; Wang, F. Q.; Yuan, Y. C.; Lin, F.; Huang, H. H.; Zhao, J. Q. High refractive index and flame retardancy of epoxy thermoset cured by tris (2-mercaptoethyl) phosphate. *Polym. Degrad. Stab.***2016**, *129*, 7-11.

(32) Gottlieb, H. E.; Kotlyar, V.; Nudelman, A. NMR chemical shifts of common laboratory solvents as trace impurities. *J. Org. Chem.* **1997**, *62*, 7512–7515.

(33) Tan,Y.; Shao, Z. B.; Yu, L. X.; Xu, Y. J.; Rao, W. H.; Chen, L. and Wang, Y. Z. Polyethyleneimine modified ammonium polyphosphate toward polyamine-hardener for epoxy resin: Thermal stability, flame retardance and smoke suppression. *Polym. Degrad. Stab.* **2016**, *131*, 62-70.

(34) Xu, Y. J.; Wang, J.; Tan, Y.; Qi, M.; Chen, L.; Wang, Y. Z. A novel and feasible approach for one-pack flame-retardant epoxy resin with long pot life and fast curing. *Chem. Eng. J.* **2018**, *337*, 30-39.

(35) Wan, J. T.; Gan, B.; Li, C.; Molina-Aldareguia, J.; Li, Z.; Wang, X.; Wang, D. Y. A novel biobased epoxy resin with high mechanical stiffness and low flammability: synthesis, characterization and properties. *J. Mater. Chem. A* **2015**, *3*, 21907-21921.

(36) Rahman, M. M.; Hosur, M.; Ludwick, A. G.; Zainuddin, S.; Kumar, A.; Trovillion, J. and Jeelani, S. Thermo-mechanical behavior of epoxy composites modified with reactive polyol diluent and randomly-oriented amino-functionalized multi-walled carbon nanotubes. *Polym. Test.* **2012**, *31*, 777-784.

(37) Bai, Y. W.; Wang, X. D.; Wu, D. Z. Novel Cyclolinear Cyclotriphosphazene-Linked Epoxy Resin for Halogen-Free Fire Resistance: Synthesis, Characterization, and Flammability Characteristic. *Ind. Eng. Chem. Res.* **2012**, *51*, 15064-15074.

(38) Yan, Y. W.; Chen, L.; Jian, R. K.; Kong, S.; Wang, Y. Z. Intumescence: An effect way to flame retardance and smoke suppression for polystyrene. *Polym. Degrad. Stab*. **2012**, 97, 1423-1431.

(39) Breulet, H.; Steenhuizen, T. Fire testing of cables: comparison of SBI with FIPEC/Europacable test. *Polym. Degrad. Stab.* **2005**, *88*, 150-158.

(40) Katsoulis, C.; Kandare, E.; Kandola, B. K. Thermal and fire performance of flame-retarded epoxy resin: investigating interaction between resorcinol bis (diphenyl phosphate) and epoxy nanocomposites. *Fire Retardancy of Polymers–New Strategies and Mechanisms* **2009**, 184-205.

(41) Jousset, S. and Catala, J. M. Peculiar Behavior of â-Phosphonylated Nitroxides Bearing a tert-octyl Group during Living/Controlled Radical Polymerization of Styrene: Kinetics and ESR Studies. *Macromolecules* **2000**, *33*, 4705-4710.

(42) Camino, G.; Costa, L.; Trossarelli, L. Study of the mechanism of intumescence in fire retardant polymers: Part V-Mechanism of formation of gaseous products in the thermal degradation of ammonium polyphosphate. *Polym. Degrad. Stab.* **1985**, *12*, 203-211.

(43) Shao, Z. B.; Deng, C.; Tan, Y.; Yu, L.; Chen, M. J.; Chen, L.; Wang, Y. Z. Ammonium polyphosphate chemically-modified with ethanolamine as an efficient intumescent flame retardant for polypropylene. *J. Mater. Chem. A* **2014**, *2*, 13955-13965.

(44) Shao, Z. B.; Deng, C.; Tan, Y.; Chen, M. J.; Chen, L.; Wang, Y. Z. Flame retardation of polypropylene via a novel intumescent flame retardant: ethylenediamine-modified ammonium polyphosphate. *Polym. Degrad. Stab*. **2014**, *106*, 88-96.

(45) Wang, X.; Zhou, S.; Xing, W. Y.; Yu, B.; Feng, X. M.; Song, L. and Hu, Y. Self-assembly of Ni–Fe layered double hydroxide/ graphene hybrids for reducing fire hazard in epoxy composites. *J. Mater. Chem. A* **2013**, *1*, 4383-4390.

(46) Wang, X.; Hu, Y.; Song, L., Xing, W. Y.; Lu, H. D.; Lv, P.; Jie, G. X. Flame retardancy

and thermal degradation mechanism of epoxy resin composites based on a DOPO substituted organophosphorus oligomer. *Polymer* **2010**, *51*, 2435-2445.

(47) Chen, M. J.; Xu, Y. J.; Rao, W. H.; Huang, J. Q.; Wang, X. L.; Chen, L.; Wang, Y. Z. Influence of Valence and Structure of Phosphorus-Containing Melamine Salts on the Decomposition and Fire Behaviors of Flexible Polyurethane Foams. *Ind. Eng. Chem. Res.* **2014**, *53*, 8773-8783.

Highlights

- A novel multi-functional polymeric curing agent for epoxy resin.
- Efficient curing ability, good flame retardancy, and high transparency.
- The mechanisms of flame retardance and transparence.